

# UCSF

## UC San Francisco Previously Published Works

### Title

Inhibitors of Pseudomonas homoserine lactones

### Permalink

<https://escholarship.org/uc/item/3jc0413g>

### Journal

Cellular Microbiology, 16(1)

### ISSN

1462-5814

### Authors

Valentine, Cathleen D  
Zhang, Hua  
Phuan, Puay-Wah  
et al.

### Publication Date

2014

### DOI

10.1111/cmi.12176

Peer reviewed

Published in final edited form as:

*Cell Microbiol.* 2014 January ; 16(1): 1–14. doi:10.1111/cmi.12176.

## SMALL MOLECULE SCREEN YIELDS INHIBITORS OF PSEUDOMONAS HOMOSERINE LACTONE-INDUCED HOST RESPONSES

Cathleen D. Valentine, Hua Zhang, Puay-Wah Phuan, Juliane Nguyen<sup>2,3</sup>, A.S. Verkman, and Peter M. Haggie

Division of Nephrology, Department of Medicine, University of California San Francisco, San Francisco, CA 94143

### SUMMARY

*P. aeruginosa* infections are commonly associated with cystic fibrosis, pneumonias, neutropenia and burns. The *P. aeruginosa* quorum sensing molecule *N*-(3-oxo-dodecanoyl) homoserine lactone (C12) cause multiple deleterious host responses, including repression of NF- $\kappa$ B transcriptional activity and apoptosis. Inhibition of C12-mediated host responses is predicted to reduce *P. aeruginosa* virulence. We report here a novel, host-targeted approach for potential adjunctive anti-*Pseudomonas* therapy based on inhibition of C12-mediated host responses. A high-throughput screen was developed to identify C12 inhibitors that restore NF- $\kappa$ B activity in C12-treated, lipopolysaccharide (LPS)-stimulated cells. Triazolo[4,3-*a*]quinolines with nanomolar potency were identified as C12-inhibitors that restored NF- $\kappa$ B-dependent luciferase expression in LPS- and TNF-stimulated cell lines. In primary macrophages and fibroblasts, triazolo[4,3-*a*]quinolines inhibited C12 action to restore cytokine secretion in LPS-stimulated cells. Serendipitously, in the absence of an inflammatory stimulus, triazolo[4,3-*a*]quinolines prevented C12-mediated responses, including cytotoxicity, elevation of cytoplasmic calcium, and p38 MAPK phosphorylation. *In vivo* efficacy was demonstrated in a murine model of dermal inflammation involving intradermal C12 administration. The discovery of triazolo[4,3-*a*]quinolines provides a pharmacological tool to investigate C12-mediated host responses, and a potential host-targeted anti-*Pseudomonas* therapy.

### INTRODUCTION

Infections by the opportunistic pathogen *P. aeruginosa* are associated with significant morbidity and mortality and constitute a significant health care burden (Restrepo and Anzueto, 2009; Craven, 2006; Gaynes *et al.*, 2005). *P. aeruginosa* is the most-frequently isolated Gram-negative bacterium in nosocomial infections and causes acute blood, lung, intra-abdominal space, urogenital tract and wound / burn infections (Fujitani *et al.*, 2011; Jones, 2010; Gaynes *et al.*, 2005). Chronic conditions are also associated with *P. aeruginosa* infection, including cystic fibrosis (CF), chronic obstructive pulmonary disease, acquired immunodeficiency syndrome, non-CF bronchiectasis and situations requiring use of indwelling catheters (Huang *et al.*, 2010; Bilton, 2008; Murray *et al.*, 2007). Antimicrobials are the mainstay of current therapy for *P. aeruginosa* infections; however, new anti-*Pseudomonas* approaches are needed because: (i) infections are often unresponsive; (ii) pan-

Address correspondence to: Peter M. Haggie, peter.haggie@ucsf.edu, tel. 415-76-8530, fax. 415-665-3847.

<sup>2</sup>Department of Bioengineering and Therapeutic Sciences, University of California San Francisco, San Francisco, CA, 94143

<sup>3</sup>Current address, Department of Pharmaceutical Sciences, School of Pharmacy and Pharmaceutical Sciences, SUNY, Buffalo, NY, 14260

drug-resistant *P. aeruginosa* strains have been isolated; and (iii) biofilms formed by *P. aeruginosa* are highly drug-resistant (Ho *et al.*, 2010; Page and Heim, 2009; Giamarellou and Kanellakopoulou, 2008).

*P. aeruginosa* employs quorum sensing to detect cell density and regulate growth, biofilm formation and expression of virulence factors (Camilli and Bassler, 2006; Lazdunski *et al.*, 2004). A major quorum sensing molecule secreted by *P. aeruginosa*, *N*-(3-oxo-dodecanoyl) homoserine lactone (C12), also influences host cells (Rumbaugh and Kaufmann, 2012). C12 inhibits activation of immune responses regulated by the NF- $\kappa$ B (nuclear factor  $\kappa$ -light chain-enhancer of activated B cells) transcription factor; a pathway that coordinates processes such as recruitment of immune cells and nitric oxide synthesis that are critical to the resolution of *P. aeruginosa* infections (Gellatly and Hancock, 2013; Mijares *et al.*, 2011; Kravchenko *et al.*, 2008; Ramphal *et al.*, 2008; Skerrett *et al.*, 2007; Feuillet *et al.*, 2006; Ramphal *et al.*, 2005; Ritchie *et al.*, 2005; Skerrett *et al.*, 2004). C12 has direct cytotoxic effects in multiple cell types including macrophages, neutrophils, fibroblasts and epithelial cells (Schwarzer *et al.*, 2012; Kravchenko *et al.*, 2006; Shiner *et al.*, 2006; Li *et al.*, 2004; Tateda *et al.*, 2003). C12 also perturbs calcium homeostasis and activates stress response pathways, including phosphorylation of p38 mitogen activated protein kinase (MAPK), phosphorylation of eukaryotic translation initiation factor 2 $\alpha$  (eIF2 $\alpha$ ), and synthesis of *c-jun* mRNA (Schwarzer *et al.*, 2010; Kravchenko *et al.*, 2006).

The concentration of C12 required to suppress NF- $\kappa$ B activity and cause apoptosis in cell cultures (~10–25  $\mu$ M) is comparable to that in *P. aeruginosa* liquid cultures and well below that in biofilms (5–600  $\mu$ M); however, evidence has been reported that lower concentrations of C12 produce responses *in vivo* (Kravchenko *et al.*, 2008; Kravchenko *et al.*, 2006; Erickson *et al.*, 2002; Smith *et al.*, 2002; Charlton *et al.*, 2000; Singh *et al.*, 2000). We hypothesized that C12-initiated host responses are key determinants of *P. aeruginosa* virulence and that inhibition of C12 activity may be therapeutically beneficial. Here, a cell-based high-throughput screen was implemented to discover small molecules that restore NF- $\kappa$ B transcriptional activity in the presence of C12. Triazolo[4,3-*a*]quinolines were identified that restored NF- $\kappa$ B-induced transcriptional and translational responses in cell lines and primary cell cultures. In addition, triazolo[4,3-*a*]quinolines inhibited several other host cell responses caused by C12, including caspase activation and Ca<sup>2+</sup>-mobilization.

## RESULTS

### Inhibitors of C12 activity identified by high-throughput screening

Subversion of NF- $\kappa$ B transcriptional responses by C12 has been demonstrated *in vivo* (Kravchenko *et al.*, 2008), which motivated our search for small molecules that could inhibit C12 activity to restore activation of NF- $\kappa$ B in the presence of an inflammatory stimulus. A cell-based phenotypic assay was employed to discover C12-inhibitors as shown schematically in Figure 1A. Under basal condition, NF- $\kappa$ B transcription is nearly inactive (Fig. 1A, *top*). Treatment of cells with an inflammatory stimulus, such as lipopolysaccharide (LPS), initiates NF- $\kappa$ B transcription, whereas stimulation of cells with LPS plus C12 does not activate NF- $\kappa$ B due to the inhibitory effects of C12 (Fig. 1A).

Screening was performed to identify small molecules that inhibit C12 activity to restore stimulated NF- $\kappa$ B transcription (Fig. 1A, *bottom*). A Fisher rat thyroid (FRT) epithelial cell line expressing a luciferase reporter under the control of an NF- $\kappa$ B response element (FRT-NF- $\kappa$ B cells) was used for high throughput screening. Cells were stimulated with LPS derived from *P. aeruginosa*; this ligand is a well-defined Toll-like receptor 4 (TLR4) agonist that induces NF- $\kappa$ B transcriptional activity and is present during *P. aeruginosa* infection. Incubation of FRT-NF- $\kappa$ B cells with LPS for 4 hours produced a luminescence response that

was ~6-fold greater than control levels (Fig. 1B). The LPS-induced luciferase expression was largely repressed by 20  $\mu\text{M}$  C12 under conditions producing little (< 5%) cell loss. Cell treatment with C12-alone did not produce NF- $\kappa$ B-stimulated luciferase expression, confirming that C12 does not produce an intrinsic response mediated by NF- $\kappa$ B (Kravchenko *et al.*, 2008; Kravchenko *et al.*, 2006). For high throughput screening, cells in test wells of 96-well plates were treated with LPS plus C12 (NF- $\kappa$ B repressed) together with test compounds (at 25  $\mu\text{M}$ ) from a small molecule library; screening plates also contained control wells in which cells were untreated, or treated with LPS or LPS plus C12. Active compounds were defined as compounds that yielded NF- $\kappa$ B-stimulated luciferase expression equal to that produced by LPS-alone stimulation. Screening of 25,600 synthetic, drug-like small molecules identified four active compounds of two chemical classes. The 2-thienotriazolo[4,3-*a*]quinoline TQ01 (Fig. 1C) had a similar core structure to compounds previously used *in vivo* as anticonvulsants; compounds in this class are orally available, have good pharmacological properties, and are synthesized readily for follow-on combinatorial chemistry (Guo *et al.*, 2009; Guan *et al.*, 2008). Further work was done with TQ01 and related analogs.

### Restoration of NF- $\kappa$ B-stimulated luciferase activity by TQ01 in distinct cell types

The inhibitory effect of C12 on NF- $\kappa$ B-stimulated luciferase expression in FRT-NF- $\kappa$ B cells was prevented by TQ01 with  $\text{IC}_{50}$  ~2.5  $\mu\text{M}$ , with complete restoration of luciferase activity at higher TQ01 concentrations (Fig. 1D). To investigate whether TQ01 action is specific for LPS-mediated NF- $\kappa$ B stimulation, FRT-NF- $\kappa$ B cells were treated with TNF (tumor necrosis factor), which also activates NF- $\kappa$ B. As with LPS, TNF-mediated NF- $\kappa$ B-stimulated luciferase expression was inhibited by C12 and the response was restored by TQ01 (Fig. 1E, *left*). TQ01 activity was also tested in RAW264.7 macrophage-like cells expressing the luciferase-based NF- $\kappa$ B reporter (RAW-NF- $\kappa$ B cells). Incubation of RAW-NF- $\kappa$ B cells for 2 hours with LPS produced an NF- $\kappa$ B-mediated luciferase response that was repressed by C12 and restored by TQ01; treatment of RAW-NF- $\kappa$ B cells with C12 did not stimulate luciferase expression (Fig. 1F, *left*). In control experiments, treatment of FRT-NF- $\kappa$ B or RAW-NF- $\kappa$ B cells with TQ01 alone did not increase NF- $\kappa$ B-stimulated luciferase activity, indicating that TQ01 does not itself stimulate inflammatory responses (Fig. 1E and 1F, *right panels*). Addition of TQ01 to LPS- or TNF-stimulated FRT-NF- $\kappa$ B cells did not enhance NF- $\kappa$ B-dependent luciferase responses, indicating that TQ01 does not merely amplify inflammatory responses initiated by NF- $\kappa$ B agonists (Fig. 1E, *right*). Similar results were obtained in LPS-stimulated RAW-NF- $\kappa$ B cells (Fig. 1F, *right*). Finally, treatment of FRT-NF- $\kappa$ B cells with C12 and TQ01 together did not activate NF- $\kappa$ B-stimulated luciferase expression (Fig. 1E, *right*). TQ01 thus inhibits C12 activity to restore NF- $\kappa$ B-driven luciferase expression in multiple cell types.

### Structure-activity studies identify potent triazolo[4,3-*a*]quinoline C12 inhibitors

Testing of 480 commercially available triazolo[4,3-*a*]quinoline analogs yielded 8 compounds with potency similar to or better than TQ01 (Table 1). The most potent compounds, TQ416 and TQ443 (Fig. 2A), fully restored NF- $\kappa$ B transcriptional responses in LPS-stimulated FRT-NF- $\kappa$ B cells with  $\text{IC}_{50}$  ~400 and 800 nM, respectively (Fig. 2B). As found for TQ01, TQ416 and TQ443 (at 10  $\mu\text{M}$ ) did not activate NF- $\kappa$ B-stimulated luciferase responses, enhance LPS-mediated NF- $\kappa$ B-stimulated luciferase activity, or act with C12 to produce an NF- $\kappa$ B response in FRT-NF- $\kappa$ B cells (Fig. 2C). Figure 2D summarizes structure-activity data for triazolo[4,3-*a*]quinolines. For the R<sup>1</sup> substitution on the quinoline ring, only methyl- and non-substituted analogs were tested in this study; non-substituted analogs were relatively inactive (e.g. TQ450 versus TQ449) and substitution at the 7- and 9-positions on the quinoline ring appeared to be more crucial than on the 4- and 5-positions (e.g. TQ456 versus TQ416). For R<sup>2</sup> substituents: aryl-methyl or aryl-ethyl groups produced

the most active compound (TQ416 and TQ443); aryl-keto-methyl groups showed moderate activity (e.g. TQ353, TQ357 and TQ371 versus TQ471); and alkyl-keto-methyl and aryl-amido-methyl groups were typically inactive (with the exception of TQ350). Triazolo[4,3-*a*]quinolines are thus potent inhibitors of C12 activity that restore NF- $\kappa$ B-mediated luciferase expression in response to activation of the NF- $\kappa$ B transcription factor.

### Triazolo[4,3-*a*]quinoline inhibition of C12 to restore NF- $\kappa$ B translational responses

Studies were performed to investigate whether TQ416, the most potent triazolo[4,3-*a*]quinoline, could restore NF- $\kappa$ B-mediated cytokine secretion. LPS stimulation of FRT cells resulted in secretion of CINC-1 (cytokine-induced neutrophil chemoattractant-1); C12 repressed CINC-1 secretion and TQ416 inhibited C12 to restore secretion (Fig. 3A). Incubation of FRT cells with C12 or TQ416 did not increase CINC-1 secretion. Stimulation of primary murine embryonic fibroblasts (MEFs) with LPS resulted in secretion of KC (keratinocyte chemoattractant) and MIP-2 (macrophage inflammatory protein-2) (Fig. 3B). C12 repressed LPS-induced KC and MIP-2 secretion from MEFs and repression was prevented by TQ416. Secretion of KC and MIP-2 was not found in MEFs that were treated with C12 or TQ416.

Experiments were also done in primary bone marrow derived macrophages (BMDM) (Fig. 3C). As in other cells types, LPS-stimulated secretion of cytokines (including TNF, RANTES (Regulated on Activation, Normal T cell Expressed and Secreted), MIP-1 $\alpha$  and IP10 (Interferon- $\gamma$ -induced protein 10)) was inhibited by C12, although TQ416 inhibited C12 to restore cytokine production. Control experiments verified that treatment of BMDM with C12 or TQ416 did not activate cytokine secretion (Supplemental Figure 1). In all cell types studied, LPS-induced cytokine levels were not significantly different from those in cells treated with LPS, C12 and TQ416. TQ416 thus inhibits C12 activity to restore physiologically relevant NF- $\kappa$ B-mediated translation responses in multiple cell lines and primary cultures.

### Triazolo[4,3-*a*]quinoline inhibition of C12 responses independent of NF- $\kappa$ B stimulation

As described in the Introduction, C12 activates multiple host cell responses. Experiments were done to determine whether TQ416 alters C12-mediated cellular signaling. Levels of *c-jun* mRNA have been reported to increase in a sustained manner in C12-stimulated BMDM, MEFs and epithelial cells (Kravchenko *et al.*, 2006). We found that C12 treatment of FRT cells for 2 hours produced an ~2-fold increase in c-Jun protein; C12-mediated c-Jun increase was not inhibited by TQ416 (Figs. 4A and 4B, *left*). Similar results were found for RAW cells and primary MEFs (Fig. 4B). In all cell types studied TQ416 did not alter c-Jun levels. C12 treatment of cells also results in transient (over ~45 minute) phosphorylation of eIF2 $\alpha$  (Kravchenko *et al.*, 2006). In FRT cells, RAW cells and MEFs, 45-minute treatment with C12 increased phosphorylated eIF2 $\alpha$  (p-eIF2 $\alpha$ ) and this response was largely unaffected by TQ416 (Fig. 4C). In control experiments, treatment of cells with TQ416 did not alter levels of p-eIF2 $\alpha$  and cell treatments did not alter levels of eIF2 $\alpha$  in FRT cells over the duration of experiments. Thus, TQ416 does not affect C12-mediated synthesis of c-Jun or phosphorylation of eIF2 $\alpha$ . A known function of p-eIF2 $\alpha$  is to inhibit protein synthesis (Samuel, 1993). TQ416 treatment of cells inhibits C12 and restores synthesis of luciferase (Figs. 1 and 2) and cytokines (Fig. 3); however, TQ416 did not alter C12-mediated transient phosphorylation of eIF2 $\alpha$  (Fig. 4). We interpret this data to indicate that the degree or duration of C12-stimulated eIF2 $\alpha$  phosphorylation is insufficient to significantly alter translation of NF- $\kappa$ B-dependent gene products.

Phosphorylation of p38 MAPK is another prominent C12-induced stress response (Kravchenko *et al.*, 2006). Treatment of FRT cells for 90 minutes with C12 increased

phosphorylated p38 MAPK (p-p38 MAPK) (Fig. 4D). In contrast to the C12-mediated cellular responses described above, phosphorylation of p38 MAPK was inhibited by TQ416. Similar C12-mediated increases in p-p38 MAPK were found in RAW cells and primary MEFs, and these responses were inhibited by TQ416. Treatment of FRT cells, RAW cells and MEFs with TQ416 did not alter p-p38 MAPK levels and p38 MAPK levels in FRT cells were not altered by treatments over the duration of experiments. Stimulation of FRT cells with LPS for 15 minutes also increased p-p38 MAPK; however, this response was not inhibited by TQ416 (Fig. 4E). These studies indicate that TQ416 inhibits the action of C12 to prevent phosphorylation of p38 MAPK, and that the inhibitory effect of TQ416 on p38 MAPK phosphorylation is not general for all stimuli.

### Triazolo[4,3-a]quinoline prevention of C12-induced cell death

Cytotoxicity is a major cellular response caused by C12 (Schwarzer *et al.*, 2012; Kravchenko *et al.*, 2006; Shiner *et al.*, 2006; Li *et al.*, 2004; Tateda *et al.*, 2003). Although C12 sensitivity is cell type-dependent, activation of caspases is a common and readily assessable feature (Schwarzer *et al.*, 2012; Kravchenko *et al.*, 2006; Tateda *et al.*, 2003). Treatment of FRT cells with 25  $\mu\text{M}$  C12 for 4 hours resulted in robust activation of the executioner caspases, caspase 3 and 7 (casp 3/7); remarkably, caspase activity was inhibited by 1  $\mu\text{M}$  TQ416 (Fig. 5A). Treatment of FRT cells with 50  $\mu\text{M}$  C12 produced significantly higher levels of casp 3/7 activation, which was inhibited ~80 % by 1  $\mu\text{M}$  TQ416. To verify TQ416 efficacy at preventing C12-mediated cytotoxicity, FRT cells were labelled with calcein and ethidium homodimer-1, stains that identify viable cells (green) and cells that have lost plasma membrane integrity (red) (Fig. 5B). C12 produced dose-dependent cell loss and increase in the number of non-viable (red fluorescent) cells; TQ416 largely prevented C12-mediated loss of cell viability (Fig. 5B and 5C).

In RAW cells, casp 3/7 activation produced by 25  $\mu\text{M}$  C12 was fully inhibited by 1  $\mu\text{M}$  TQ416 (Fig. 5D); however, 3  $\mu\text{M}$  TQ416 was needed to inhibit casp 3/7 activation initiated by 40  $\mu\text{M}$  C12. Finally, casp 3/7 activation upon treatment of primary MEFs with 25  $\mu\text{M}$  C12 was inhibited by ~95 % with 3  $\mu\text{M}$  TQ416 and ~70 % with 1  $\mu\text{M}$  TQ416. In all cell types studied, TQ416 did not activate casp 3/7 or cause cytotoxicity over 24 hours (data not shown). In control experiments, TQ416 did not prevent casp 3/7 activation in RAW cells treated with anisomycin or staurosporine for 6 hours (Fig. 5E). These studies indicate the TQ416 prevents C12-mediated caspase activation and suggest that this inhibitory effect is not general for all apoptotic stimuli.

### Efficacy of triazolo[4,3-a]quinolines in an *in vivo* model of dermal inflammation

Experiments were performed to investigate the *in vivo* efficacy of TQ416 using a murine model of dermal inflammation involving intradermal C12 administration. Intradermal injection of C12-loaded micelles, but not control micelles, produced local immune cell infiltration, as assessed by hematoxylin and eosin staining and immunohistological analysis of skin sections excised 24 hours post injection (Fig. 6 and Supplemental Fig. 2). Immune cell infiltration was greatly reduced when TQ416 was injected together with C12. Injection of TQ416 alone did not cause cell infiltration. TQ416 thus prevents C12-induced intradermal immune cell infiltration.

### Rapid triazolo[4,3-a]quinoline inhibition of C12-mediated responses

A rapid, readily quantifiable response observed in C12-stimulated cells is release of  $\text{Ca}^{2+}$  from the endoplasmic reticulum (ER) (Schwarzer *et al.*, 2010; Shiner *et al.*, 2006). As expected, stimulation of SV40-immortalized MEFs (wt MEFs) with C12 produced a robust increase in cytoplasmic  $\text{Ca}^{2+}$  as detected using Fluo-4 (Fig. 7 and Supplementary Fig. 3A). The increase in cytoplasmic  $\text{Ca}^{2+}$  in C12-treated wt MEFs was prevented by TQ416. In

control experiments, treatment of cells with TQ416 did not alter cytoplasmic  $\text{Ca}^{2+}$ , nor did it alter  $\text{Ca}^{2+}$  responses caused by ATP or thapsigargin (TG) (Fig. 7A, *inset*, and 7B). Studies in FRT cells and primary MEFs also showed TQ416 inhibition of C12-mediated elevation in cytoplasmic  $\text{Ca}^{2+}$  (Supplemental Figs. 3B and 3C). TQ416 thus acts rapidly to prevent C12-mediated cellular responses.

### Triazolo[4,3-*a*]quinoline inhibition of XBP1s-dependent and -independent C12 caspase activation

We previously demonstrated that the X-box binding protein 1 transcription factor (XBP1s) is a key determinant of C12-mediated caspase activation (Valentine *et al.*, 2013). Generation of mature, XBP1s-encoding mRNA requires non-conventional splicing of a pre-mRNA (*Xbp1u*) by the inositol-requiring enzyme 1 $\alpha$  (IRE1 $\alpha$ ) endoribonuclease (Lee *et al.*, 2002). Compared to control cells (wt MEFs), C12-mediated casp 3/7 activation is greatly reduced (~90 %) in cells that cannot generate XBP1s (*Ire1 $\alpha$ <sup>-/-</sup>* MEFs) or do not possess the *Xbp1* gene (*Xbp1<sup>-/-</sup>* MEFs); this finding was interpreted to indicate that C12 activates caspases via XBP1s-dependent (~90 %) and XBP1s-independent pathways (~10 %). As expected, treatment of wt MEF with TQ416 resulted in near-complete suppression of C12-mediated casp 3/7 activation (Fig. 7C, *black*). In *Ire1 $\alpha$ <sup>-/-</sup>* MEFs, which activate caspases via the minor XBP1s-independent pathway, TQ416 completely inhibited casp 3/7 activation. These experiments indicate that TQ416 inhibits caspase activation produced by XBP1s-dependent and -independent pathways.

## DISCUSSION

Infections by *P. aeruginosa* occur in acute and chronic settings, most commonly in pneumonias, burns, wounds, CF and in conditions requiring in-dwelling catheters (Restrepo and Anzueto, 2009; Craven, 2006; Gaynes *et al.*, 2005). New approaches are required to combat *P. aeruginosa* infections primarily because *P. aeruginosa* has evolved multiple mechanisms to reduce antimicrobial efficacy (Page and Heim, 2009). Prevention of C12-mediated host effects represents a potential target for anti-*Pseudomonas* therapies (Kravchenko and Kaufmann, 2013; Rumbaugh and Kaufmann, 2012). The goal of this study was to discover small-molecule inhibitors of C12 that restore NF- $\kappa$ B-mediated transcriptional responses with the objective of applying these compounds to investigate C12-host cell interactions and to establish the role of C12-mediated host responses in *P. aeruginosa* virulence.

Although C12-mediated inhibition of NF- $\kappa$ B activity and caspase activation are arguably the principal host responses of most relevance to *P. aeruginosa* virulence, little is known about how distinct C12-mediated cellular responses are interrelated (Rumbaugh and Kaufmann, 2012). In addition to restoring NF- $\kappa$ B activity, TQ416 prevented C12-mediated caspase activation, p38 MAPK phosphorylation and  $\text{Ca}^{2+}$  release from the ER. Control experiments suggested that TQ416 inhibits C12 responses selectively; albeit with the caveat that our survey of alternative stimuli was not exhaustive. At a cell biological level, we classify C12-mediated host responses as triazolo[4,3-*a*]quinoline-sensitive and -insensitive processes (Fig. 7D). C12-mediated NF- $\kappa$ B repression and caspase activation are inhibited by TQ416, whereas transient phosphorylation of eIF2 $\alpha$  and synthesis of c-Jun are not. Our data thus suggest that NF- $\kappa$ B repression and caspase activation are independent of p-eIF2 $\alpha$  and c-Jun production, or that p-eIF2 $\alpha$  and c-Jun are upstream of the TQ416 site(s) of action. Restoration of stimulated luciferase expression (Figs. 1 and 2) and cytokine secretion (Fig. 3) by TQ416 suggests that inhibition of protein synthesis by p-eIF2 $\alpha$  has a minimal effect on the synthesis of NF- $\kappa$ B-dependent gene products. As such, the degree of p-eIF2 $\alpha$  production by C12 or the duration eIF2 $\alpha$  phosphorylation in C12-stimulated cells is presumably

insufficient to alter translation of NF- $\kappa$ B-dependent gene products greatly. In a prior study, we identified the XBP1s transcription factor as a key determinant of C12-mediated caspase activation (Valentine *et al.*, 2013). Phosphorylation of p38 MAPK was conserved in C12-treated XBP1s-deficient cells (*Irel1* $\alpha^{-/-}$  and *Xbp1* $^{-/-}$  MEFs) and pharmacological inhibition of p38 MAPK did not prevent C12 apoptosis, suggesting that C12-mediated caspase activation is not heavily dependent upon p-p38 MAPK activity. Phosphorylation of eIF2 $\alpha$  was also conserved in XBP1s-deficient cells, suggesting that p-eIF2 $\alpha$  generation is not a key determinant of C12-mediated caspase activation, or that XBP1s regulates caspase activity downstream of p-eIF2 $\alpha$  (Valentine *et al.*, 2013). In general, these studies suggest that major C12-mediated cellular responses (inhibition of NF- $\kappa$ B activity and caspase activation) are largely independent of p-p38 MAPK and p-eIF2 $\alpha$  activity; further work will be required to establish whether distinct host receptors mediate these different cellular signaling events.

The observation that TQ416 prevents C12-mediated NF- $\kappa$ B repression, activation of caspases, and release of ER Ca $^{2+}$  stores provides evidence to suggest that these responses may be interrelated. Perturbations in mitochondrial, ER and lysosomal Ca $^{2+}$  homeostasis leads to diverse pro-apoptotic responses (Rizzuto *et al.*, 2012; Rasola and Bernardi, 2011; Orrenius *et al.*, 2003). A limited number of reports have indicated that Ca $^{2+}$  mobilization is also required for NF- $\kappa$ B activation (Chun and Prince, 2006; Check *et al.*, 2010; Tauseef *et al.*, 2012). We speculate that ER Ca $^{2+}$  release elicited by C12 is central to downstream actions on host cell signaling pathways. Further work is required to elucidate mechanisms by which C12 mobilizes ER Ca $^{2+}$ , how perturbation of cellular Ca $^{2+}$  relates to C12-mediated host responses, and how triazolo[4,3-*a*]quinolines prevent C12-mediated Ca $^{2+}$  mobilization.

An original motivation for this study was to discover small molecule C12 inhibitors to investigate the hypothesis that C12-mediated host effects enhance *P. aeruginosa* virulence. Skin wounds and burns are frequently infected by *P. aeruginosa*; therefore, we employed a murine model in which C12 was injected into the dermis to examine *in vivo* efficacy of triazolo[4,3-*a*]quinolines. Whereas injection of C12 produced local infiltration of immune cells to the dermis, administration of C12 plus TQ416 inhibited the inflammatory response, and TQ416 alone did not alter skin morphology or induce inflammation. The pattern of immune cell infiltration observed in the dermis after C12 injection is similar with that seen during repair of cutaneous wounds (including excisional, incisional, implant and chemical wound models) (Kolaczowska and Kubes, 2013; Brancato and Albina, 2011). Based on the known cytotoxic activity of C12 (e.g., see Kravchenko *et al.*, 2006 and Fig. 5), the absence of direct C12 immunostimulatory activity (Kravchenko *et al.*, 2008 and Figs. 1, 2 and 3) and the pattern of immune cell infiltration observed, we interpret our data to indicate that C12-induced cytotoxicity stimulates immune cell infiltration (as in other wounds) and that TQ416 inhibits C12-mediated cytotoxicity *in vivo*. As such, the skin studies demonstrate that TQ416 can inhibit C12-mediated responses *in vivo*. Further work using clinically relevant *P. aeruginosa* infection models will be required to establish the efficacy of triazolo[4,3-*a*]quinolines in preventing C12-mediated host responses and reducing *P. aeruginosa* virulence.

In summary, a cell-based high throughput screen was employed to identify triazolo[4,3-*a*]quinolines as small molecule C12-inhibitors that restore NF- $\kappa$ B immune responses in stimulated cells. In the absence of an inflammatory stimulus, triazolo[4,3-*a*]quinolines also prevent C12-mediated caspase activation, release of ER Ca $^{2+}$ , and phosphorylation of p38 MAPK kinase. Prevention of major C12-mediated host effects, including repression of NF- $\kappa$ B signaling and apoptosis, is predicted to reduce *P. aeruginosa* virulence. Testing of triazolo[4,3-*a*]quinolines in murine models of *P. aeruginosa* infection is warranted and demonstration that triazolo[4,3-*a*]quinolines reduce *P. aeruginosa* virulence could lead to the development of a novel, host-targeted, adjunctive anti-*Pseudomonas* therapy.



## EXPERIMENTAL PROCEDURES

### Cell culture

Fisher rat thyroid (FRT) cells were maintained in Ham's F12 medium supplemented with 5 % FBS, 2 mM glutamine, 100 units/ml penicillin, 0.1 mg/ml streptomycin, and non-essential amino acids. To generate an NF- $\kappa$ B reporter cell line, cells were transfected with pGL4.32[*luc2P/NF- $\kappa$ B-RE/HYGRO*] (Promega) and enriched by repeated culture in medium containing 0.25 mg/ml hygromycin. RAW264.7 murine macrophage-like cells were cultured in DMEM-H21 supplemented with 10 % FBS, 2 mM glutamine, 100 units/ml penicillin, 0.1 mg/ml streptomycin, and non-essential amino acids. To generate an NF- $\kappa$ B reporter cell line, cells were transfected with pGL4.32[*luc2P/NF- $\kappa$ B-RE/HYGRO*] and enriched by repeated culture using medium supplemented with 0.1 mg/ml hygromycin. Primary MEFs were purchased from Lonza and cultured according to the manufacturer's instructions. BMDM were cultured as previously described (Kravchenko *et al.*, 2006). Control (wild type) and *Irela* -deficient SV40-immortalized MEFs were previously described (Valentine *et al.*, 2013).

### High-throughput screening and assays of NF- $\kappa$ B-stimulated luciferase expression

FRT NF- $\kappa$ B reporter cells were cultured for 24 hours in white, clear-bottom 96-well luminescence plates (Greiner) using 100  $\mu$ l medium per well. Additions of *P. aeruginosa* LPS (500 ng/ml, Sigma-Aldrich), C12 (20  $\mu$ M, Sigma-Aldrich) and test compounds (4 per well, each at 25  $\mu$ M, ChemDiv) to plates were made using a Biomek liquid handling system. In each plate, 4 wells contained control cells, 4 wells contained LPS-alone, 8 wells contained LPS and C12 and 80 wells contained LPS, C12 and test compounds. Cells were incubated at 37 °C in 5 % CO<sub>2</sub> for 4 hours prior to addition of 100  $\mu$ l Bright-Glo luciferase assay substrate and detection of luminescence signal with a BMG FLUOStar OPTIMA plate reader. The z-factor for this assay was typically >0.7. Additional assays of NF- $\kappa$ B-stimulated luciferase expression in FRT-NF- $\kappa$ B and RAW-NF- $\kappa$ B cells were performed in 96-well format as described above. For NF- $\kappa$ B reporter assays, the concentrations of C12 and timing of assays were chosen such that C12-mediated cell loss was typically <10 % during the course of experiments. Concentrations of reagents and duration of experiments used to assess NF- $\kappa$ B transcriptional activity are provided in the Results, Figures or Figure Legends. Data from luminescence assays is presented as mean  $\pm$  s.d., with data derived from 6–8 wells, and is representative of at least duplicate experiments. Triazolo[4,3-*a*]quinoline analogs used for secondary screening were purchased from ChemDiv.

### Analysis of cytokines

Cells were cultured using standard conditions with the exception of primary MEFs that were serum starved as described (Kravchenko *et al.*, 2008). Cytokines produced by stimulated FRT cells and BMDM were initially identified using Proteome Profiler Cytokine Array Panels (R&D Systems). Quantitative analysis of cytokine levels was performed with a MAGPIX and appropriate MagPlex Microspheres for individual or multiplexed analytes (Invitrogen). Concentrations of LPS, C12 and TQ416 used in experiments are provided in Figure Legend 3. Data is presented as mean  $\pm$  s.d. with data derived from 3–6 individual cell cultures.

### Immunostaining and immunoblotting

Antibodies against c-Jun, p38 MAPK, phosphorylated p38 MAPK, eIF2 $\alpha$  and phosphorylated eIF2 $\alpha$  were purchased from Cell Signaling. Immunofluorescence studies were performed on fixed and permeabilized cells using anti-c-Jun antibody (1:500), fluorophore-conjugated anti-rabbit secondary antibody (1:500; Invitrogen) and DAPI

(Invitrogen) as a counter-stain. Fluorescence imaging was performed using a Nikon TE2000 microscope equipped with a Hamamatsu C9100 EM-CCD, Exfo X-Cite light source, appropriate filter cube, and objective lens (Nikon S Fluor 20× N.A. 0.75). Quantitative analysis of area-integrated, background-corrected fluorescence intensity associated with individual cells was performed using ImageJ. Data is presented as mean ± s.e.m. and was compiled from at least three individual cell cultures per experimental maneuver, with >20 cells analyzed per image. Immunoblotting was performed using standard procedures, antibody dilutions suggested by vendors and data is representative of at least duplicate experiments. For these experiments, C12-mediated cell death was negligible over the duration of experiments (45–120 minutes).

### Assessment of C12-mediated caspase activation and cytotoxicity

Caspase 3/7 activity was measured using the Caspase-Glo 3/7 homogeneous luminescent assay (Promega). Normalized data is presented as mean ± s.d., was derived from 6–12 individual measurements and is representative of at least duplicate experiments. C12-mediated cytotoxicity was assessed using the LIVE/DEAD cell viability assay (Invitrogen) that stains viable cells with calcein and non-viable cells with ethidium homodimer-1. Quantitative analysis of C12-mediated cytotoxicity was based on analysis of background-corrected, integrated fluorescence area of calcein fluorescence before and after C12-treatment. For experiments in RAW cells, staurosporine and anisomycin were purchased from Tocris.

### In vivo studies

Micelles were prepared by adding test compounds (DMSO control, C12, C12 plus TQ416 and TQ416) to mPEG-2000 (1,2-dioleoyl-sn-glycero-3-phosphoethanolamine-N-[methoxy(polyethylene glycol)-2000]) (Avanti Polar Lipids) dissolved in chloroform. Solvents were removed by rotary evaporation and the compound-lipid mixture was further dried under vacuum prior to rehydration in Hepes-buffered saline (HBS; 20 mM Hepes, 150 mM NaCl, pH 7.4) and sonication to generate micelles. Preparations contained 1.71 mg mPEG-2000 and 10 µg of TQ416 and / or C12 per 50 µl of HBS. C57BL/6 mice were prepared for subcutaneous injection in the back by shaving and 15 µl injections were made with a 30-gauge needle. Each mouse studied was injected two-times (on each side of the back) with control, C12-, C12 plus TQ416- and TQ416-loaded micelles. Mice were sacrificed 24 hours post injection and skin was removed, fixed (4 % paraformaldehyde) and embedded in paraffin. For histological analysis, 5 µm tissue sections were stained with hematoxylin and eosin using standard procedures. For immunohistochemistry, 5 µm tissue sections were deparaffinized and stained with primary antibody prior to secondary detection using VECTASTAIN Elite ABC Kit and DAB Peroxidase Substrate Kit (Vector Lab). Primary antibodies used were rat anti-CD45 (BD Biosciences), rat anti-Ly6G (eBioscience) and rat anti-F4/80 (eBioscience). Imaging was performed using a Leica DM4000B microscope equipped with Spot RTKE CCD camera and appropriate objective lenses (10× N.A. 0.3 and 20× N.A. 0.5 air and 63× N.A. 1.25 oil immersion lens). Analysis of inflammatory cell infiltration was performed on images of the dermis using ImageJ. Images were converted to 8-bit format, binarized and a histogram of pixel intensities generated to calculate the fraction of pixels that contain inflammatory cells (Supplemental Fig. 2D).

### Calcium signaling

Measurements of cytosolic Ca<sup>2+</sup>-responses were made using cells labelled with Fluo-4 NW as directed by the manufacturer (Invitrogen). Measurements were made at room temperature and fluorescence images were acquired using a Nikon TE2000 microscope equipped with a Hamamatsu C9100 EM-CCD, Exfo X-Cite light source, 31001 filter cube, Nikon S Fluor 20× N.A. 0.75 objective lens and shuttered illumination (12 Hz). Data analysis was

performed using Wasabi (Hamamatsu); raw data is presented as mean, background-corrected, area-integrated fluorescence intensity averaged from 4–6 areas of 3–6 cells and data summaries represent mean  $\pm$  s.e.m. from 3–7 experimental repeats per maneuver.

## Supplementary Material

Refer to Web version on PubMed Central for supplementary material.

## Acknowledgments

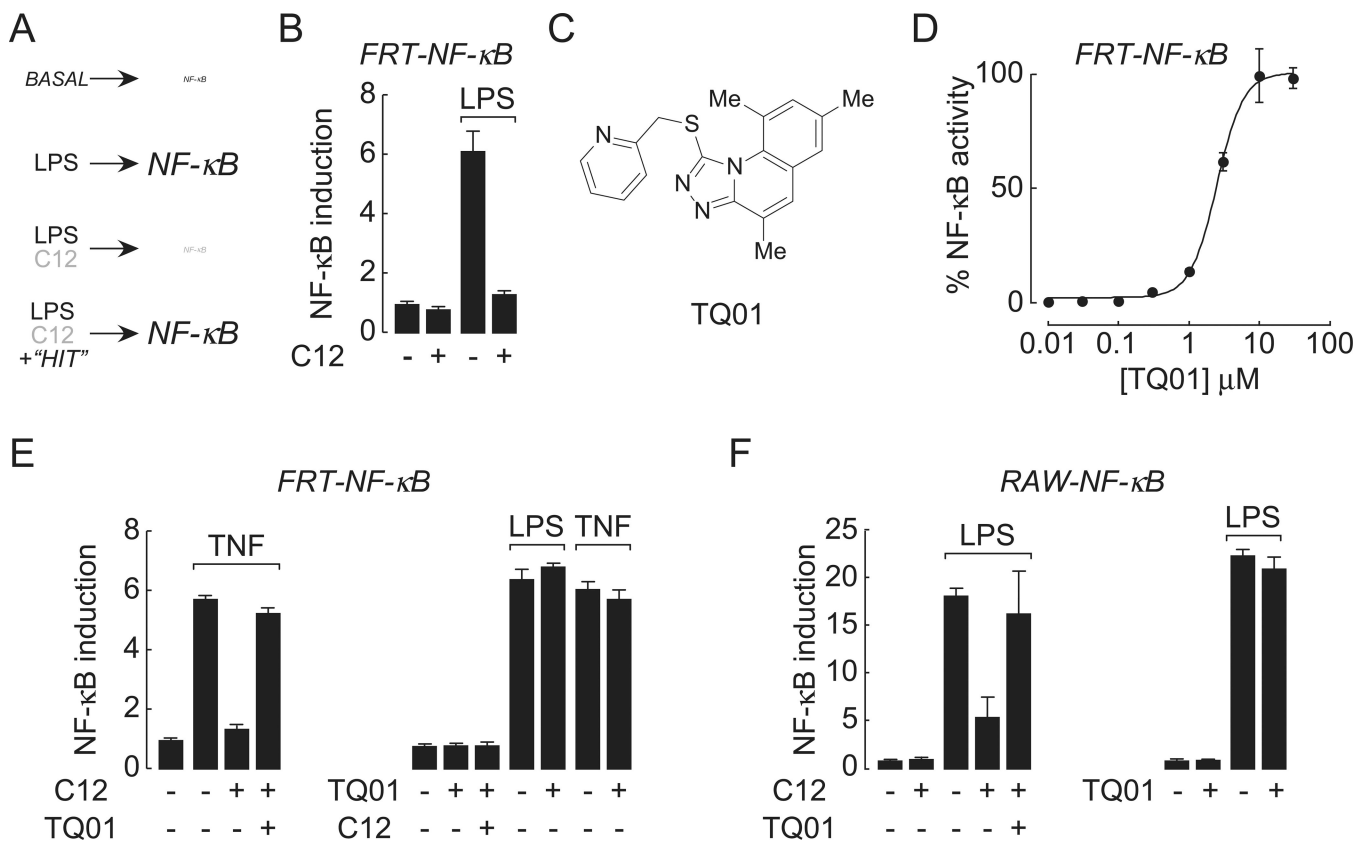
These studies were funded by awards DK081355 (PMH) and DK072517 (ASV is the Program Director and PMH received a Pilot Award) from the NIDDK, and a Research Development Program grant (R613) from the Cystic Fibrosis Foundation (ASV and PMH). The authors wish to thank Drs. Francis Szoka, Scott Oakes, Feroz Papa and Joanne Engel (UCSF) and Jonathon Koff (Yale) for their helpful discussion during this project.

## REFERENCES

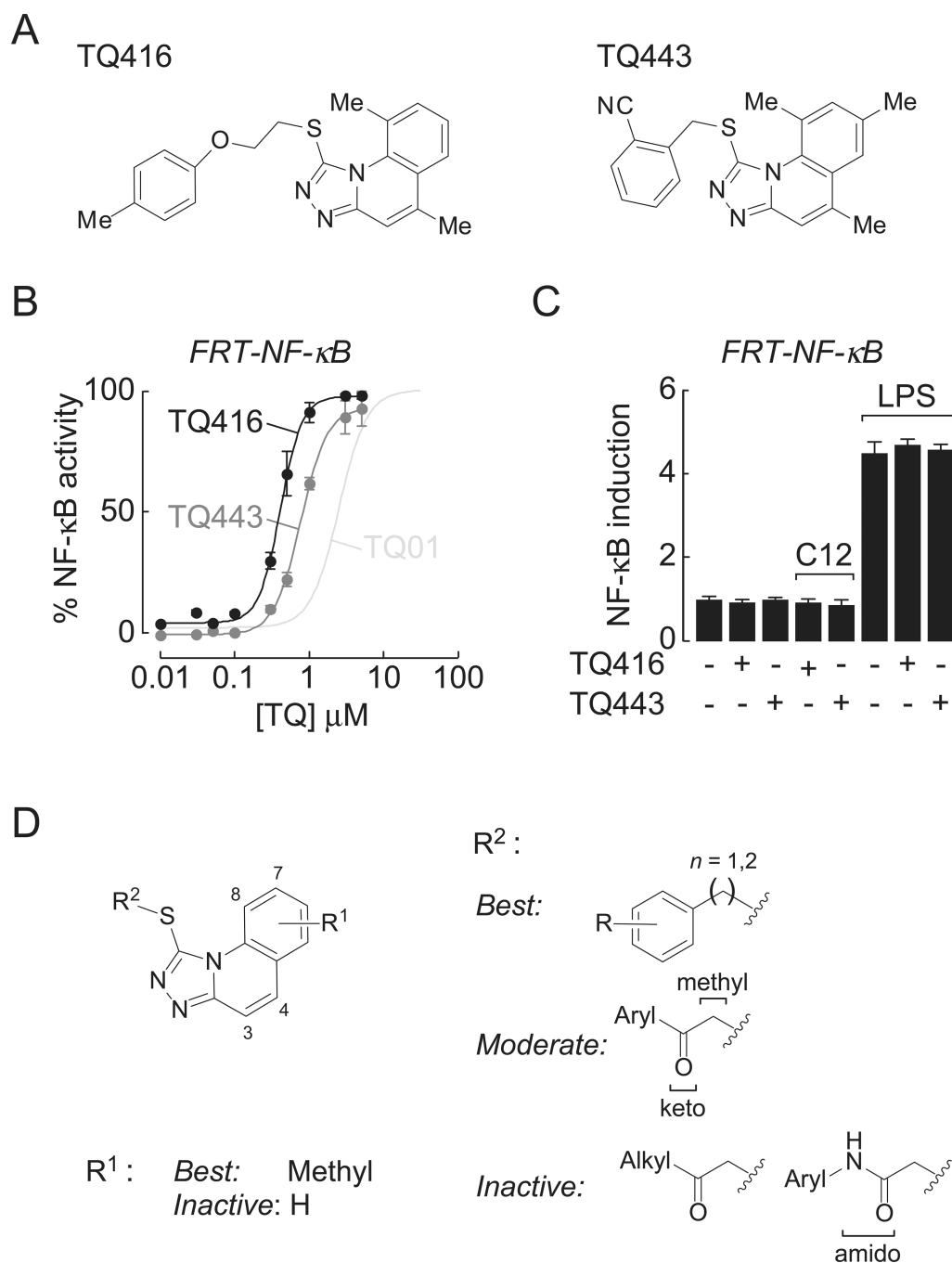
- Bilton D. Update on non-cystic fibrosis bronchiectasis. *Curr Opin Pulm Med*. 2008; 14:595–599. [PubMed: 18812838]
- Brancato SK, Albina JE. Wound macrophages as a key regulator of repair: origin, phenotype, and function. *Am J Pathol*. 2011; 178:19–25. [PubMed: 21224038]
- Camilli A, Bassler BL. Bacterial small-molecule signaling pathways. *Science*. 2006; 311:1113–1116. [PubMed: 16497924]
- Charlton TS, de Nys R, Netting A, Kumar N, Hentzer M, Givskov M, Kjelleberg S. A novel and sensitive method for the quantification of *N*-3-oxoacyl homoserine lactones using gas chromatography-mass spectroscopy: application to a model of bacterial biofilm. *Environ Microbiol*. 2000; 2:530–541. [PubMed: 11233161]
- Check J, Byrd CL, Menio J, Rippe RA, Hines IN, Wheeler MD. Src kinase participates in LPS-induced activation of NADPH oxidase. *Mol Immunol*. 2010; 47:756–762. [PubMed: 19942291]
- Chun J, Prince A. Activation of Ca<sup>2+</sup>-dependent signaling by TLR2. *J Immunol*. 2006; 177:1330–1337. [PubMed: 16818794]
- Craven DE. What is healthcare-associated pneumonia, and how should it be treated? *Curr Opin Infect Dis*. 2006; 19:153–160. [PubMed: 16514340]
- Erickson DL, Endersby R, Kirkham A, Stuber K, Vollman DD, Rabin HR, et al. *Pseudomonas aeruginosa* quorum-sensing systems may control virulence factor expression in the lungs of patients with cystic fibrosis. *Infect Immun*. 2002; 70:1783–1790. [PubMed: 11895939]
- Feuillet V, Medjane S, Mondor I, Demaria O, Pagni PP, Galan JE, et al. Involvement of Toll-like receptor 5 in the recognition of flagellated bacteria. *Proc Natl Acad Sci USA*. 2006; 103:12487–12492. [PubMed: 16891416]
- Fujitani S, Sun H-Y, Yu VL, Weingarten JA. Pneumonia due to *Pseudomonas aeruginosa*, Part I. *Chest*. 2011; 139:909–919. [PubMed: 21467058]
- Gaynes R, Edwards JR. Overview of Nosocomial infections caused by Gram-negative Bacilli. *Clin Infect Dis*. 2005; 15:389–391. [PubMed: 16392087]
- Gellatly SL, Hancock RE. *Pseudomonas aeruginosa*: new insights into pathogenesis and host defenses. *Pathogens and Disease*. 2013; 67:159–173. [PubMed: 23620179]
- Giamarellou H, Kanellakopoulou K. Current therapies for *Pseudomonas aeruginosa*. *Crit Care Clin*. 2008; 24:261–278. [PubMed: 18361945]
- Guan L-P, Jin Q-H, Wang S-F, Li F-N, Quan Z-S. Synthesis and anticonvulsant activity of 5-phenyl-[1,2,4]-triazolo[4,3-*a*]quinolines. *Arch Pharm Chem Life Sci*. 2008; 341:774–779.
- Guo L-J, Wei C-X, Jia J-H, Zhao L-M, Quan Z-S. Design and synthesis of 5-alkoyl-[1,2,4]triazolo[4,3-*a*]quinoline derivatives with anticonvulsant activity. *Eur J Med Chem*. 2009; 44:954–958. [PubMed: 18752871]
- Ho J, Tambyah PA, Paterson DL. Multiresistant Gram-negative infections: a global perspective. *Curr Opin Infect Dis*. 2010; 23:546–553. [PubMed: 20802331]

- Huang YJ, Kim E, Cox MJ, Brodie EL, Brown R, Weiner-Kronish JP, Lynch SV. A persistent and diverse microbiota present during chronic obstructive pulmonary disease exacerbations. *OMICS*. 2010; 14:9–59. [PubMed: 20141328]
- Jones RN. Microbial etiologies of hospital-acquired bacterial pneumonia and ventilator-associated bacterial pneumonia. *Clin Infect Dis*. 2010; 51:S81–S87. [PubMed: 20597676]
- Kolaczowska E, Kubes P. Neutrophil recruitment and function in health and inflammation. *Nat Rev Immunol*. 2013; 13:159–175. [PubMed: 23435331]
- Kravchenko VV, Kaufmann GF. Bacterial inhibition of inflammatory responses via TLR-independent mechanisms. *Cell Microbiol*. 2013; 15:527–536.
- Kravchenko VV, Kaufmann GF, Mathison JC, Scott DA, Katz AZ, Grauer DC, et al. Modulation of gene expression via disruption of NF- $\kappa$ B signaling by bacterial small molecules. *Science*. 2008; 321:259–263. [PubMed: 18566250]
- Kravchenko VV, Kaufmann GF, Mathison JC, Scott DA, Katz AZ, Wood MR, et al. *N*-(3-Oxo-acyl)homoserine lactones signal cell activation through a mechanism distinct from canonical pathogen-associated molecular pattern recognition receptor pathways. *J Biol Chem*. 2006; 281:28822–28830. [PubMed: 16893899]
- Lazdunski A, Ventre I, Sturgis JN. Regulatory circuits and communication in gram-negative bacteria. *Nat Rev Immunol*. 2004; 2:581–592.
- Lee K, Tirasophon W, Shen X, Michalak M, Prywes R, Okada T, et al. IRE1-mediated unconventional mRNA splicing and SP2-mediated ATF6 cleavage merge to regulate XBP1 in signaling the unfolded protein response. *Genes Dev*. 2002; 16:452–466. [PubMed: 11850408]
- Li L, Hooi D, Chhabra SR, Pritchard D, Shaw PE. Bacterial *N*-acylhomoserine lactone-induced apoptosis in breast carcinoma cells correlated with down-modulation of STAT3. *Oncogene*. 2004; 23:4894–4902. [PubMed: 15064716]
- Mijares LA, Wangdi T, Sokol C, Homer R, Medzhitov R, Kazmierczak BI. Airway epithelial MyD88 restores control of *Pseudomonas aeruginosa* murine infection via an IL-1-dependent pathway. *J Immunol*. 2011; 186:7080–7088. [PubMed: 21572023]
- Murray TS, Egan M, Kazmierczak BI. *Pseudomonas aeruginosa* chronic colonization in cystic fibrosis patients. *Curr Opin Pediatr*. 2007; 19:83–88. [PubMed: 17224667]
- Orrenius S, Zhivotovsky B, Nicotera P. Regulation of cell death: the calcium-apoptosis link. *Nat Rev Mol Cell Biol*. 2003; 4:552–565. [PubMed: 12838338]
- Page MGP, Heim J. Prospects for the next anti-*Pseudomonas* drug. *Curr Opin Pharm*. 2009; 9:558–565.
- Ramphal R, Balloy V, Huerre M, Si-Tahar M, Chignard M. TLRs 2 and 4 are not involved in hypersensitivity to acute *Pseudomonas aeruginosa* lung infections. *J Immunol*. 2005; 175:3927–3934. [PubMed: 16148139]
- Ramphal R, Balloy V, Jyot J, Verma A, Si-Tehar M, Chignard M. Control of *Pseudomonas aeruginosa* in the lung requires the recognition of either lipopolysaccharide or flagellin. *J Immunol*. 2008; 181:586–592. [PubMed: 18566425]
- Rasola A, Bernardi P. Mitochondrial permeability transition in Ca<sup>2+</sup>-dependent apoptosis and necrosis. *Cell Calcium*. 2011; 50:222–233. [PubMed: 21601280]
- Restrepo MI, Anzueto A. The role of gram-negative bacteria in healthcare-associated pneumonia. *Semin Respir Crit Care Med*. 2009; 30:61–66. [PubMed: 19199188]
- Ritchie AJ, Jansson A, Stallberg J, Nilsson P, Lysaght P, Cooley MA. The *Pseudomonas aeruginosa* quorum-sensing molecule *N*-3-(oxododecanoyl)-1-homoserine lactone inhibits T-cell differentiation and cytokine production by a mechanism involving an early step in T-cell activation. *Infect Immun*. 2005; 73:1648–1655. [PubMed: 15731065]
- Rizzuto R, De Stefani D, Raffaello A, Mammucari C. Mitochondria as sensors and regulators of calcium signaling. *Nat Rev Mol Cell Biol*. 2012; 13:566–578. [PubMed: 22850819]
- Rumbaugh KP, Kaufmann GF. Exploitation of host signaling pathways by microbial quorum sensing signals. *Curr Opin Microbiol*. 2012; 15:162–168. [PubMed: 22204809]
- Samuel CE. The eIF-2 $\alpha$  protein kinases, regulators of translation in eukaryotes from yeast to humans. *J Biol Chem*. 1993; 268:7603–7606. [PubMed: 8096514]

- Schwarzer C, Fu Z, Patanwala M, Hum L, Lopez-Guzman M, Illek B, et al. *Pseudomonas aeruginosa* biofilm-associated homoserine lactone C12 rapidly activates apoptosis in airway epithelia. *Cell Microbiol.* 2012; 14:698–709. [PubMed: 22233488]
- Schwarzer C, Wong S, Shi J, Matthes E, Illek B, Ianowski JP, et al. *Pseudomonas aeruginosa* homoserine lactone activates store-operated cAMP and cystic fibrosis transmembrane regulator-dependent Cl<sup>-</sup> secretion by human airway epithelia. *J Biol Chem.* 2010; 285:34850–34863. [PubMed: 20739289]
- Shiner EK, Terentyev D, Bryan A, Sennoune S, Martinez-Zaguilan R, Gyorke S, et al. *Pseudomonas aeruginosa* autoinducer modulates host cell responses through calcium signaling. *Cell Microbiol.* 2006; 8:1601–1610. [PubMed: 16984415]
- Singh PK, Schaefer AL, Parsek MR, Moninger TO, Welsh MJ, Greenberg EP. Quorum-sensing signals indicate that cystic fibrosis lungs are infected with bacterial biofilms. *Nature.* 2000; 407:762–764. [PubMed: 11048725]
- Skerrett SJ, Liggitt HD, Hajjar AM, Wilson CB. Myeloid differentiation factor 88 is essential for pulmonary host defense against *Pseudomonas aeruginosa* but not *Staphylococcus aureus*. *J Immunol.* 2004; 172:3377–3381. [PubMed: 15004134]
- Skerrett SJ, Wilson CB, Liggitt HD, Hajjar AM. Redundant Toll-like receptor signaling in pulmonary host response to *Pseudomonas aeruginosa*. *Am J Physiol Cell Mol Physiol.* 2007; 292:L312–L322.
- Smith RS, Harris SG, Phipps R, Iglewski BH. The *Pseudomonas aeruginosa* quorum-sensing molecule *N*-(3-oxododecanoyl) homoserine lactone contributes to virulence and induces inflammation *in vivo*. *J Bacteriol.* 2002; 184:1132–1139. [PubMed: 11807074]
- Tateda K, Ishii Y, Horikawa M, Matsumoto T, Miyariri S, Pechere JC, et al. The *Pseudomonas aeruginosa* autoinducer *N*-3-oxododecanoyl homoserine lactone accelerates apoptosis in macrophages and neutrophils. *Infect Immun.* 2003; 71:5785–5793. [PubMed: 14500500]
- Tauseef M, Knezevic N, Chava KR, Smith S, Sukriti S, Gianaris N, et al. TLR4 activation of TRPC6-dependent calcium signaling mediates endotoxin-induced lung vascular permeability and inflammation. *J Exp Med.* 2012; 209:1953–1968. [PubMed: 23045603]
- Valentine CD, Anderson MO, Papa FR, Haggie PM. X-Box binding protein 1 (XBP1s) is a critical determinant of *Pseudomonas aeruginosa* homoserine lactone-mediated apoptosis. *PLOS Pathogen.* 2013 In press.



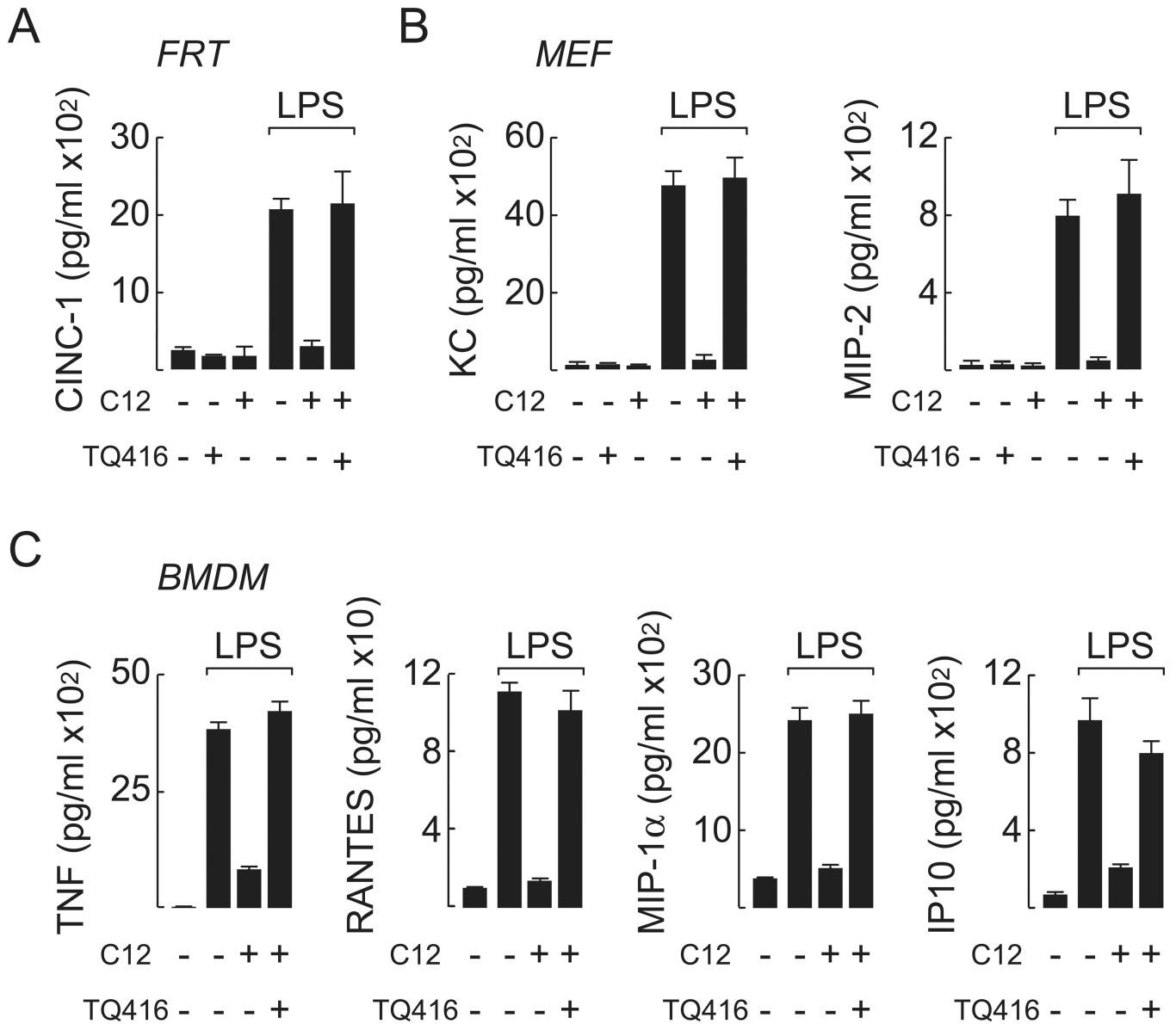
**Figure 1.** Triazolo[4,3-*a*]quinolines inhibit C12 activity to restore NF-κB-stimulated luciferase expression in LPS-stimulated cells. **A.** Schematic representation of the screening procedure. **B.** Luminescence responses of FRT-NF-κB cells; treatments were for 4 hours with LPS (500 ng/ml) and C12 (20 μM). **C.** 2-thieno-triazolo[4,3-*a*]quinoline (TQ01) structure. **D.** Dose response of normalized NF-κB-mediated luciferase activity in FRT-NF-κB cells (treatments as in **A**). **E.** (*left*) NF-κB-stimulated luciferase expression in FRT-NF-κB cells treated with TNF (50 ng/ml), C12 and TQ01 (10 μM). (*right*) TQ01 does not activate or enhance NF-κB-mediated luciferase activity, or act with C12 to elicit NF-κB responses. **F.** (*left*) NF-κB-stimulated luciferase responses in RAW-NF-κB cells treated for 2 hours with LPS (10 ng/ml), C12 (25 μM) and TQ01 (10 μM). (*right*) TQ01 does not activate or enhance NF-κB-mediated luciferase activity in RAW-NF-κB cells. Stimulated NF-κB-mediated luciferase responses were statistically relevant ( $p < 0.0001$ ) and no significant difference was found for comparison of LPS- and LPS + C12 + TQ01-stimulated cells or comparisons made in control experiments (panels *E right*, and *F right*).



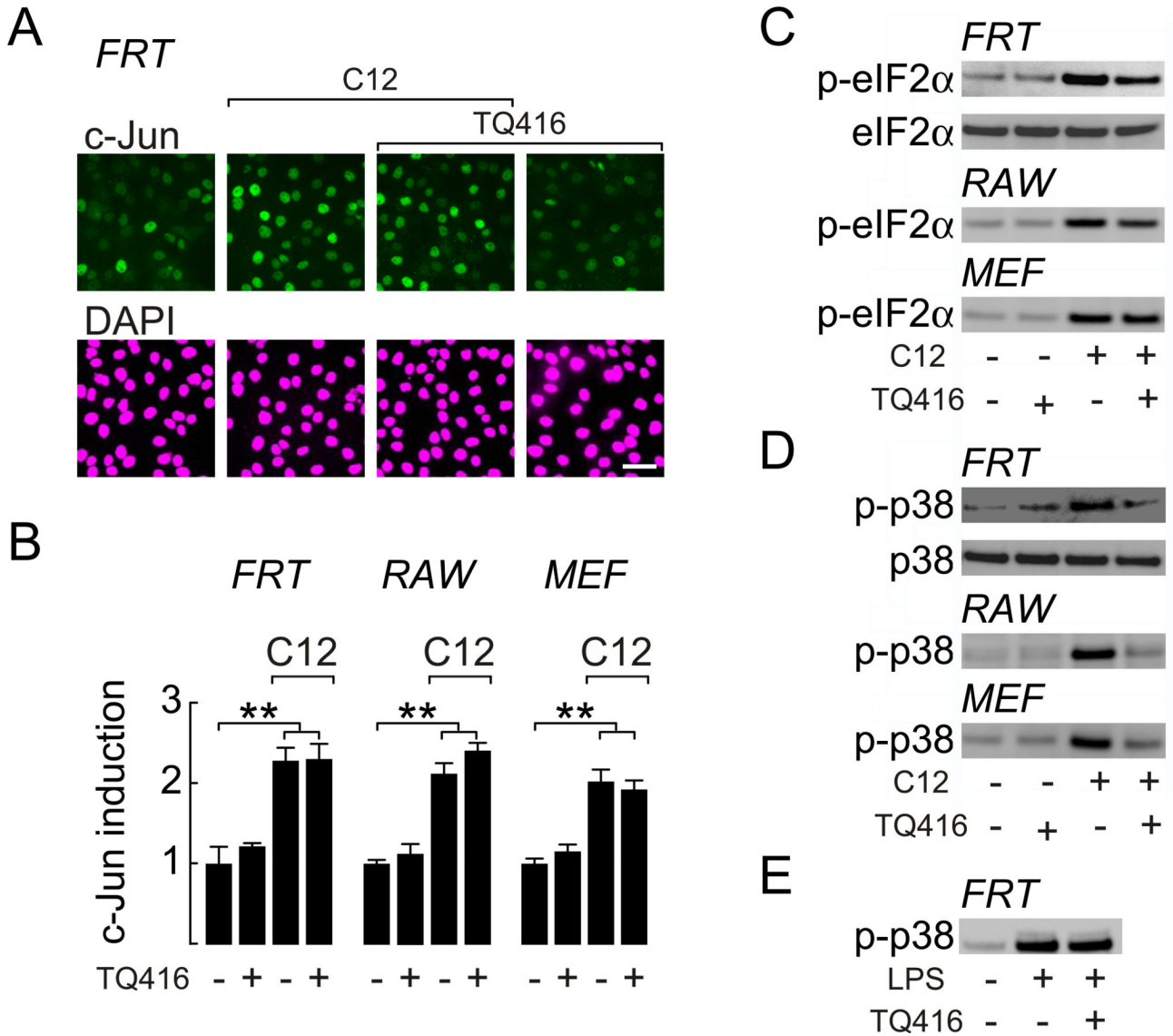
**Figure 2.** Potent triazolo[4,3-*a*]quinolines identified by secondary screening. A. TQ416 and TQ443 structures. B. Dose response of normalized NF- $\kappa$ B-mediated luciferase activity in FRT-NF- $\kappa$ B cells treated with LPS, C12 and TQ416 (black), TQ443 (dark gray) or TQ01 (light gray; curve as in Fig. 1D). C. TQ01 does not activate or enhance NF- $\kappa$ B-stimulated luciferase expression, or act with C12 to elicit NF- $\kappa$ B responses in FRT-NF- $\kappa$ B cells. D. Structural determinants of triazolo[4,3-*a*]quinoline activity: the triazolo[4,3-*a*]quinoline core structure (left, top) and substituents at the  $R^1$  (left, bottom) and  $R^2$  positions (right) are shown.

Stimulated NF- $\kappa$ B transcriptional responses were statistically relevant ( $p < 0.0001$ ) and no significant difference was found for comparisons in control experiments.

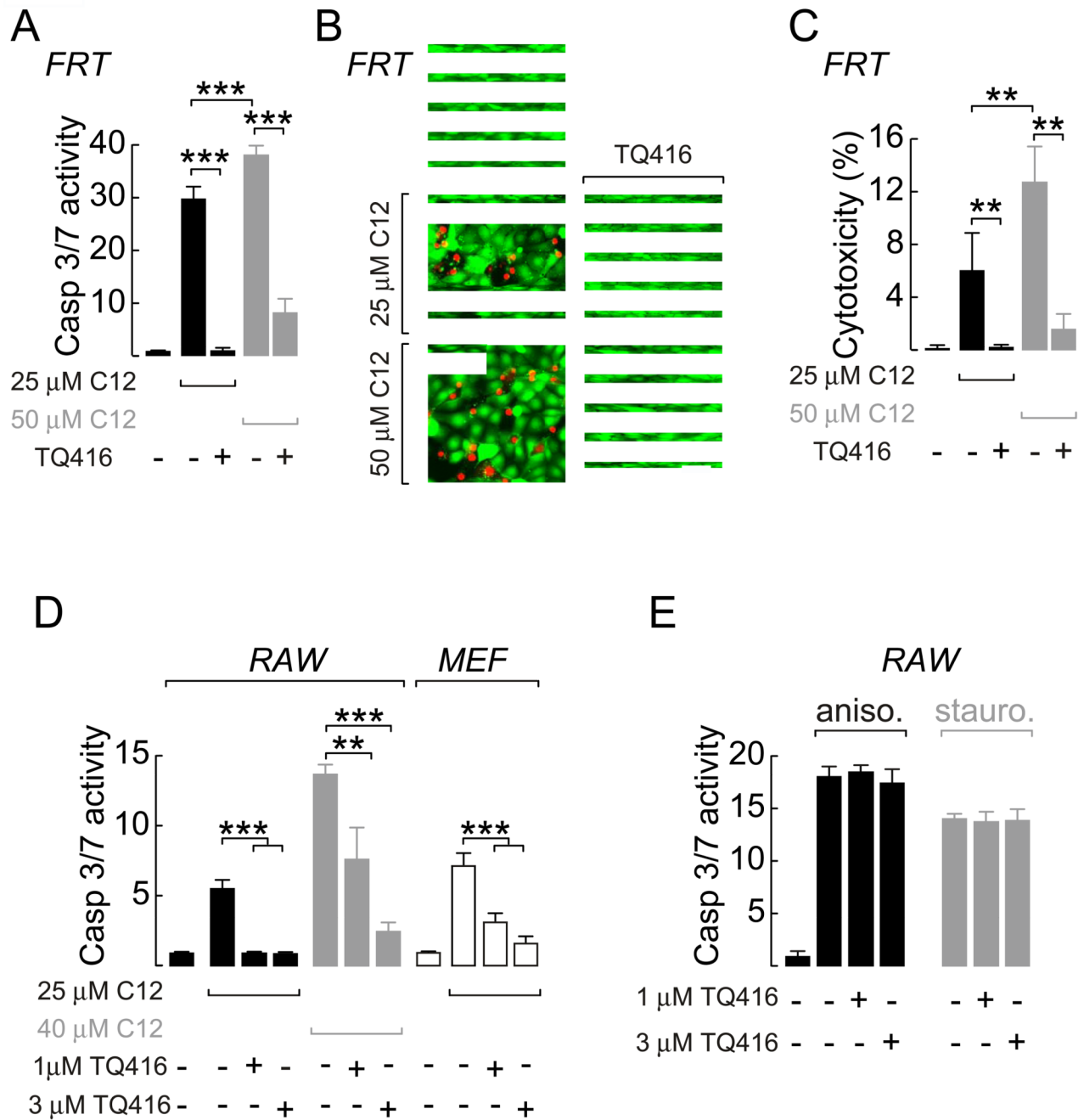


**Figure 3.**

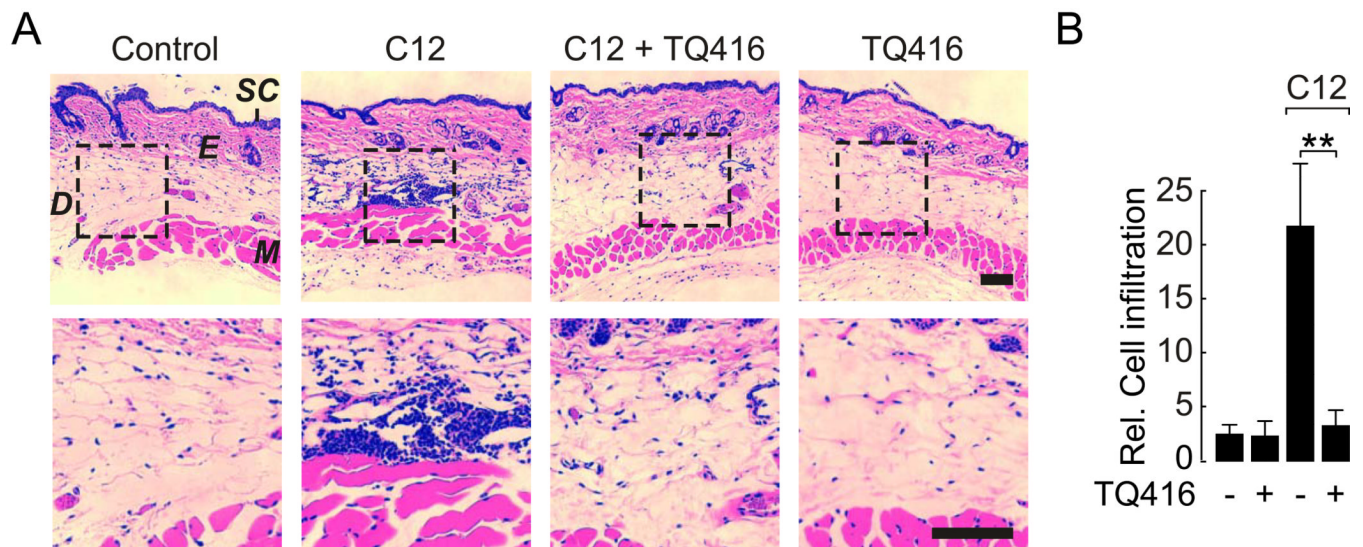
The triazolo[4,3-*a*]quinoline TQ416 inhibits C12 activity to restore NF- $\kappa$ B-mediated cytokine secretion. A. CINC-1 secretion in FRT cells. Cells were treated with LPS (500 ng/ml), C12 (25  $\mu$ M) and TQ416. B. KC (*left*) and MIP-2 (*right*) secretion in primary MEFs (treatments as in A). C. TNF (*first panel*), RANTES (*second panel*), MIP-1 $\alpha$  (*third panel*) and IP10 (*fourth panel*) secretion in BMDM. Cells were treated with LPS (10 ng/ml), C12 (25  $\mu$ M) and TQ416. In all experiments, cells were treated for 4 hours, LPS produced significant increases in cytokines ( $p < 0.0001$ ) and TQ416 was used at 1  $\mu$ M.

**Figure 4.**

The triazolo[4,3-*a*]quinoline TQ416 inhibits C12-mediated phosphorylation of p38 MAPK. A. FRT cells immunostained for c-Jun (*top*) and stained with DAPI (*bottom*) after 2 hours treatment with C12 (20  $\mu$ M) and TQ416 (scale bar, 50  $\mu$ m). B. Quantitative analysis of c-Jun levels; RAW cells and MEFs were treated for 1.5 hours. \*\*  $p < 0.005$ ; no significant difference observed for control *vs.* TQ416-treated cells or C12- *vs.* C12 plus TQ416-treated cells. C. Western blot analysis of p-eIF2 $\alpha$  and eIF2 $\alpha$  (in FRT cells; *second panel*). Cells were treated with C12 (25  $\mu$ M) and TQ416 for 45 minutes. D. Western blot analysis of p-p38 MAPK and p38 MAPK (in FRT cells; *second panel*). Cells were treated with C12 (25  $\mu$ M) and TQ416 for 1.5 hours. E. Western blot analysis of p-p38 MAPK in FRT cells treated with LPS (500 ng/ml) and TQ416 for 15 minutes. TQ416 was used at 1  $\mu$ M in all experiments.

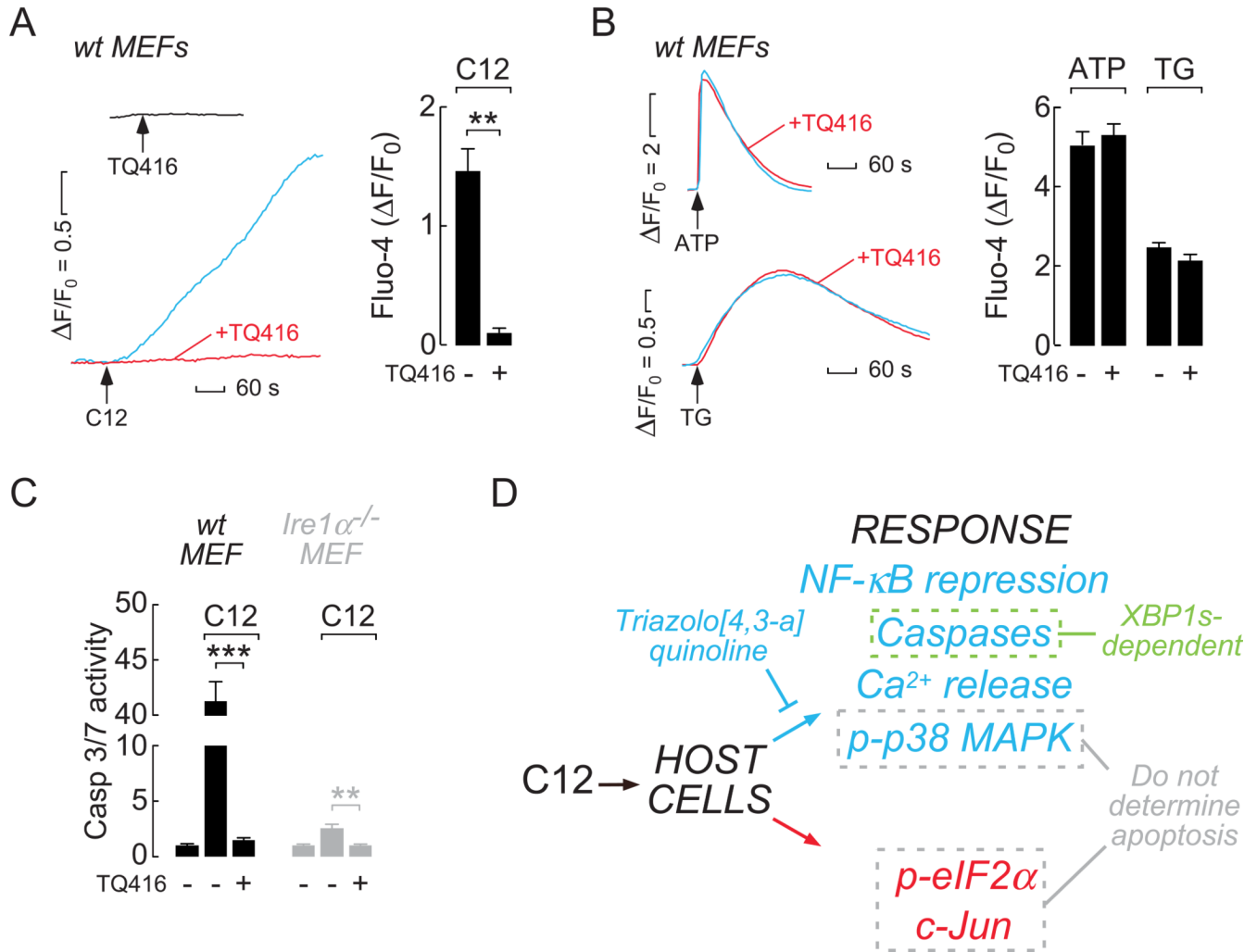
**Figure 5.**

TQ416 prevents C12-induced cytotoxicity. A. Caspase activation in FRT cells treated with C12 and TQ416 (1  $\mu$ M). B. Fluorescence images of FRT cells stained with calcein (green) and ethidium homodimer-1 (red) after C12 and TQ416 (1  $\mu$ M) treatment (scale bar, 50  $\mu$ m). C. C12-induced cytotoxicity (cell loss) in FRT cells treated with C12 and TQ416. D. TQ416 inhibits C12-induced executioner caspase activation in RAW cells (*left*; black and gray bars) and primary MEFs (*right*; empty bars). E. TQ416 does not inhibit executioner caspase activation in RAW cells treated with anisomycin (0.1 mg/ml, *black*) or staurosporine (5  $\mu$ M, *gray*). \*\*  $p < 0.005$ , \*\*\*  $p < 0.0005$ . In all experiments, cells were treated for 4 hours.



**Figure 6.**

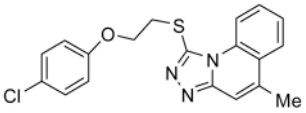
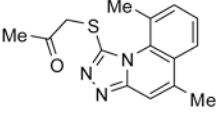
TQ416 prevents C12-induced inflammation in murine skin. A. Hematoxylin and eosin stained skin sections prepared from mice 24 hours after injection with (from left to right) control micelles and micelles containing C12, C12 plus TQ416, and TQ416. Images are shown at low magnification (*top*) and for an expanded region (*bottom*, located with dashed box at low magnification; scale bars, 100  $\mu$ m). The following regions are identified: stratum corneum (SC), epidermis (E), dermis (D) and muscle (M). B. Quantitation of immune cell infiltration to the dermis (\*\*  $p < 0.005$ ).

**Figure 7.**

Characterization of TQ416 activity. A. (left) Measurements of cytoplasmic Ca<sup>2+</sup> in wt MEFs in response to C12 (blue), C12 plus TQ416 (red) and TQ416 (inset, black). (right) Summary data for relative Ca<sup>2+</sup> increases in wt MEFs. B. (left) Ca<sup>2+</sup> measurements in wt MEFs in response to ATP (top) and thapsigargin (TG, bottom) in the absence (blue) and presence of TQ416 (red). (right) Summary data for peak relative Ca<sup>2+</sup> increase in ATP or TG stimulated wt MEFs. C. Caspase activation in wt (black) and *Ire1 $\alpha$ <sup>-/-</sup>* MEFs (gray) after 6 h treatment with C12 (25  $\mu$ M) and TQ416 (1  $\mu$ M). Statistical analysis was by t-test (\*\* p < 0.005 \*\*\* p < 0.0005). D. Cellular responses elicited by C12 can be defined as triazolo[4,3-a]quinoline-sensitive (blue) or -insensitive (red). Activation of executioner caspases is highly dependent upon XBP1s (highlighted green).

**Table 1**Structure and efficacy of active triazolo[4,3-*a*]quinolines identified.

| Compound | Structure | IC <sub>50</sub> (μM) |
|----------|-----------|-----------------------|
| TQ01     |           | 2.5                   |
| TQ416    |           | 0.4                   |
| TQ443    |           | 0.8                   |
| TQ353    |           | 1.0                   |
| TQ357    |           | 1.5                   |
| TQ371    |           | 4.0                   |
| TQ449    |           | 4.0                   |
| TQ350    |           | 10.0                  |
| TQ450    |           | > 25                  |

| Compound | Structure   | IC <sub>50</sub> (μM) |
|----------|---|-----------------------|
| TQ456    |  | > 25                  |
| TQ471    |  | > 25                  |